Title

Full: Improving emotion control in social anxiety by targeting rhythmic brain activity
Short: Dual-site tACS improves emotion control in anxiety

Authors

Sjoerd Meijer[1†*], Bob Bramson[1,2†], Ivan Toni[1‡], and Karin Roelofs[1,2‡]

Affiliations

[1]Donders Institute for Brain, Cognition and Behavior, Centre for Cognitive Neuroimaging (DCCN), Radboud University Nijmegen, 6525 EN Nijmegen, the Netherlands.

[2]Behavioral Science Institute (BSI), Radboud University Nijmegen, 6525 GD Nijmegen, the Netherlands.

[†,‡]These authors contributed equally to this work.

[*]Corresponding author.

E-mail: sjoerd.meijer@donders.ru.nl

Abstract

Social avoidance is a hallmark of social anxiety disorder. Difficulties in controlling avoidance behavior are the core maintaining factor of this impairing condition, hampering the efficacy of existing therapies. This preregistered study tested a physiologically-grounded non-invasive enhancement of control over social approach and avoidance behavior in socially anxious individuals. Their prefrontal and sensorimotor areas received dual-site phase-coupled electrical stimulation, to enhance inter-regional theta-gamma phase-amplitude coupling, a mechanism known to support emotion control in non-anxious individuals. We measured behavioral and fMRI-BOLD responses during in-phase, anti-phase, and sham stimulations, while participants performed a social approach-avoidance task, involving either automatic or controlled emotional actions. In-phase (*vs.* anti-phase) stimulation selectively enhanced control over approach-avoidance actions, and modulated neural responses in the same prefrontal region where stimulation-reactivity increased as a function of trait anxiety. These findings illustrate how human neurophysiological connectivity can be leveraged to improve control over social avoidance, opening the way for mechanistically grounded clinical interventions of persistent avoidance in anxiety disorders.

Teaser

Emotion control in social anxiety can be boosted by targeting rhythmic brain activity between prefrontal and sensorimotor cortex

Introduction

Anxiety disorders are marked by an inability to flexibly regulate prepotent approach and avoidance tendencies to adapt behavior to contextual demands. Persistent avoidance of perceived threats causes and maintains anxiety, preventing the extinction of those threats through exposure, thereby exacerbating the disorder (*1–4*). There is an urgent need for non-invasive interventions targeted at improving emotional action control in anxious individuals. Recent work has improved cognitive and behavioral functions in neurotypical individuals, boosting inter-regional neural communication through dual-site phase-amplitude-coupled transcranial alternating current stimulation (dual-site tACS) (*5–8*). This non-invasive neuromodulation technique, grounded on the physiology of directional inter-regional neuronal communication, can also enhance emotion control in non-anxious individuals (*9*). Here, we test the generalizability of this approach by applying dual-site tACS in a group of participants selected for high social anxiety, a trait known to be associated with impaired emotional action control (*10–12*). This translational test is a critical step toward developing clinically-relevant interventions for modulating emotional behavioral control.

Patients suffering from social anxiety disorder have particular difficulties in overriding automatic avoidance tendencies in social situations. Previous research has identified the lateral prefrontal cortex (lPFC) as a critical brain region involved in selecting between competing approach-avoidance actions (*13*, *14*). This control is implemented through rhythmic modulation of excitability in downstream areas, including the sensorimotor cortex (SMC) and parietal cortex (*9*, *15–17*). Specifically, successful control over social-emotional approach-avoidance actions has been linked to temporal coupling between the phase of theta-band rhythms in lPFC and the amplitude of gamma-band activity in SMC (*15–17*). Dual-site tACS offers a means to non-invasively modulate this inter-regional phase-amplitude coupling, enhancing long-range synchronization between task-relevant neural circuits (*5*, *9*, *18*). We have shown that in-phase stimulation, designed to synchronize peaks of theta-band rhythms in lPFC with the amplitude of gamma-band neural activity in SMC, improves accuracy when non-anxious participants override automatic emotional action tendencies (*9*). Given the pivotal role of the lPFC in regulating approach-avoidance actions (*19*) and the importance of theta-gamma coupling between lPFC and SMC for successful control over social-emotional approach-avoidance actions (*9*, *15*), here we test whether dual-site tACS applied to lPFC-SMC can enhance emotional action control in highly socially anxious individuals. We applied in-phase and anti-phase dual-site tACS while forty-nine highly socially anxious individuals performed an approach-avoidance task, using concurrent fMRI to quantify prefrontal engagement during control over emotional action tendencies.

Results

Emotional action control: Behavioral performance and neural activation

Forty-nine participants, selected on high self-reported social anxiety (**Fig. 1A**), were instructed to use a joystick to approach happy and avoid angry faces (affect-congruent condition) or avoid happy and approach angry faces (affect-incongruent condition) (**Fig. 1B**). The affect-incongruent condition requires participants to override automatic emotional action tendencies to avoid angry and approach happy faces (*20*, *21*). In the

baseline sham-tACS condition, expected affective congruency effects were observed, with higher error rates for incongruent as compared to congruent responses, b = .41; 95% Credible Interval (CI) [.22 .61] (*9*, *15*, *19*, *22*) (**Fig. 1C**). Effects from Bayesian Mixed Effects models were considered significant if the 95% CI did not include 0.

The patterns of neural activity largely aligned with previous findings using the same task, showing increased activation during incongruent *versus* congruent trials in bilateral parietal cortex, precuneus, and right dorsal anterior cingulate cortex, as well as decreased activity in bilateral medial and orbitofrontal cortex, parahippocampal gyrus, amygdala-hippocampus, temporal pole, and right fusiform cortex (*9*, *15*, *19*) (**Fig. 1D**). However, highly anxious individuals exhibited more robust activation for incongruent trials in the dorsolateral prefrontal cortex (dlPFC; Brodmann areas 9/46d) [30, 36, 38], rather than in the lateral frontal pole (FPl) region previously found in non-anxious individuals (*9*, *22*, *23*). The differences in emotional action control circuits between high-anxious and non-anxious individuals have been detailed in a separate paper (*24*). These findings indicate that high-anxious and non-anxious individuals show similar behavioral difficulties in controlling emotional action tendencies. Still, high-anxious individuals likely implement control using dlPFC rather than FPl (*24*).

tACS dose- and phase-dependent modulation of emotional action control

Transcranial current stimulation, when effective, modulates ongoing neural activity (*25*, *26*). Following our pre-registered analysis pipeline (https://osf.io/j9s2z), we evaluated the cerebral effects of prefrontal tACS by examining BOLD activity in the region involved in implementing emotional action control in these high-anxious participants. Given that high-anxious individuals recruit dlPFC to solve emotional action control (*24*), and that the dual-site tACS montage of this study evokes fields covering dlPFC (**Fig. 2A**), we choose dlPFC BOLD activity as a metric of tACS dose-response. As in (*9*), the tACS-dose metric is obtained from a BOLD contrast (active tACS > sham tACS) that is orthogonal to both the tACS phase manipulation (**Fig. 2B**) and the emotional action control contrast. Critically, we observe tACS-dose and tACS-phase specific enhancement of emotional action control, b = -.35; 95% CI [-.67 -.03] ([emotional action control * tACS-phase * tACS-dose dlPFC]) (**Fig. 2C**). Participants with a stronger dlPFC dose-response to tACS also exhibited greater improvement in controlling their emotional actions when receiving in-phase as opposed to anti-phase tACS. Planned post-hoc analyses confirm significant dose-dependent effects for the in-phase (Spearman's $\rho(47) = -0.37$, $p = .009$) but not for the anti-phase condition (Spearman's $\rho(47) = 0.09$, $p = .519$). The direction and magnitude of the dual-site tACS intervention effects align with our previous report (*9*). Accordingly, when extracting tACS-dose from FPl, a region previously reported to be decoupled from emotional action control in high-anxious individuals (*24*), no significant tACS-induced changes in emotional action control were observed (b = -.12; 95% CI [-.45 .23] ([emotional action control * tACS-phase * tACS-dose FPl]). Moreover, further exploration of brain-symptoms correlations revealed a positive association between higher trait anxiety levels and stronger tACS-dose in dlPFC (**Fig. 2D**). These findings demonstrate that dual-site tACS can effectively enhance emotional action control in high-anxious individuals by targeting phase-amplitude coupling between dlPFC and SMC.

Discussion

This study demonstrates that in-phase dual-site tACS, targeted at facilitating endogenous theta-gamma phase-amplitude coupling between lPFC and SMC, enhances control over emotional action tendencies in highly socially anxious individuals. The main finding is that dual-site tACS effects, previously reported to improve control over automatic approach-avoidance tendencies in non-anxious participants (*9*), generalize to a clinically relevant population with altered control over daily-life social-emotional behavior (LSAS ≥ 30) (*11*, *12*, *27*). Furthermore, this study shows that the dual-site tACS intervention in high-anxious males and females evokes effects in a different prefrontal territory (dlPFC) than in non-anxious males (FPl) (*9*). This observation fits the recently reported shift in the prefrontal circuit implementing emotional action control from FPl (non-anxious participants) to dlPFC (high-anxious participants) (*24*). The current study demonstrates the possibility of improving emotional action control using dual-site tACS in high-anxious individuals via the facilitation of endogenous long-range phase-amplitude coupling. This finding extends our mechanistic understanding of approach-avoidance control in social anxiety and introduces rhythmic synchronization between dlPFC and SMC as a novel therapeutic tool.

dlPFC-SMC phase-amplitude coupling supports emotional action control in social anxiety

This dual-site tACS intervention builds on prior studies that have demonstrated the significance of endogenous lPFC-SMC theta-gamma coupling in controlling automatic emotional action tendencies and in facilitating the implementation of alternative goal-directed actions (*9*, *15*). In this study, in-phase dual-site tACS could enhance interregional synchronization of neuronal excitability periods, biasing action selection in SMC according to valence-incongruent action goals in dlPFC (*15–17*). In one important detail, this putative mechanism differs from what has been observed in healthy individuals, where prefrontal control emerged from FPl (*9*) rather than dlPFC (this study). This difference is important for understanding the scope and the mechanism of the dual-site tACS intervention in social anxiety. Namely, FPl is a region that can flexibly integrate valence signals with approach-avoid action selection, allowing FPl to orchestrate goal-directed control over automatic emotional action tendencies (*13*, *23*). However, the FPl is overexcitable in high-anxious individuals (*24*), and the evidence suggests dlPFC compensates for FPl when control over emotional actions is required (*24*). In contrast with integrated valence-action goal representations observed in FPl, action goal representations in dlPFC are not modulated by valence (*23*), consistent with relatively limited mono-synaptic connections from amygdala to dlPFC (*28*, *29*). In fact, dlPFC engagement could dampen amygdala processing via strong indirect projections to the ventromedial subgenual cingulate area 25 (*30*, *31*), thereby providing a candidate mechanism for gating the contribution of emotional afferences to cognitive control (*32*). Thus, the dlPFC can implement rule-based actions with minimal interference from emotional valence signals even in high anxiety, when emotional signals would saturate an already overexcitable FPl (*24*). However, the scope of dlPFC-based emotional action control might be limited when emotional challenges co-occur with demands for cognitive control, e.g. during real-life situations. Accordingly, high-anxious individuals show reduced dlPFC efficiency during cognitive control compared to non-anxious individuals (*33*). It remains to be seen whether dual-site tACS in socially-anxious individuals can enhance dlPFC coordination with SMC

and remain behaviorally effective even in the presence of multiple cognitive control demands.

tACS BOLD dose-response in dlPFC scales with trait anxiety

The current study shows that the application of in-phase dual-site tACS results in behavioral effects proportional to the dlPFC BOLD signal evoked across stimulation conditions by the prefrontal tACS electrode, i.e., a dose-response effect. This finding corresponds to the observation that high-anxious individuals recruit the dlPFC when instructed to control automatic emotional action tendencies (*24*). We also observe that individuals with higher trait anxiety exhibit more robust dlPFC responses to the tACS intervention. This finding corresponds to the observation that trait anxiety is associated with an anatomical shift of prefrontal emotional action control, from FPl to dlPFC (*24*). The link between tACS response and trait anxiety signals that sub-optimal endogenous synchronization could underlie reduced emotion control performance in anxiety. Namely, the most robust effects of tACS are expected when weaker endogenous oscillations can be facilitated (*34*), and in-phase dual-site tACS is expected to improve long-range communication by reducing noise within hypo-synchronized circuits (*35*). Specifically, we suggest that trait anxiety might index individual levels of neural noise within the dlPFC-SMC circuit during emotional action control, a prediction that could be tested by measuring electrophysiological activity during emotional action control in high-anxious individuals (*15*). This knowledge would be instrumental in facilitating the translation of dual-site tACS to clinical protocols, as it would enable using trait anxiety rather than concurrent tACS-fMRI to estimate individual dose-responses.

Interpretational issues and future directions

It could be argued that the current findings are limited by the lack of direct observations on tACS-induced rhythmic adjustments. In fact, the manipulation of dual-site tACS phase angle (in-phase *versus* anti-phase) enables us to relate the tACS effects to phase-specific changes in long-range phase-amplitude coupling, and exclude general changes in lPFC or SMC excitability. The phase manipulation provides the additional benefit of fully matching peripheral effects between in-phase and anti-phase stimulation, thereby ruling out alternative explanations related to transcutaneous entrainment or retinal stimulation (*36*, *37*).

In this study, phase-specific dual-site tACS improvements in emotional action control are dose-related, which suggests high inter-individual variation in the effects of dual-site tACS on emotional action control. This variation makes the tACS effects physiologically plausible, since this is expected as variation in the neurophysiological response to tACS effects depends on the electric field induced in the brain (*38*, *39*) and on the interaction with ongoing oscillations (*34*). This variation signals the need to identify factors that could maximize intervention response. Future studies could use individualized current flow models to optimize stimulation protocols and enhance targeting accuracy to achieve more consistent tACS effects (*40*). However, these models do not capture state-dependent effects in the neural response to stimulation (*41*), which could be particularly relevant for translational efforts in which the neural mechanisms underlying the disorder are not fully understood. Furthermore, it is important to note that the dual-site tACS intervention is not intended to be a standalone treatment, but rather to enhance the effectiveness of existing treatments. This can

include improving the ability to control emotional behavior during exposure therapy to confront threatening situations and temporarily interrupt the cycle of persistent avoidance. Hence, studying how existing treatments interact with our neuromodulation intervention in clinical settings is essential.

Building non-invasive neuromodulation interventions that facilitate a cognitive function presents a major neuroscientific challenge due to the need to identify and enhance the underlying endogenous neural dynamics. Translating mechanistically-informed neuromodulation interventions from healthy individuals to clinical populations poses a further challenge, due to incomplete understanding of the neural mechanisms underlying psychiatric disorders. Here, we successfully translate a mechanistically informed dual-site tACS intervention (*9*, *15*) to a clinically relevant high-anxiety population that shows impairments in daily-life social-emotional behavior. The findings highlight the advantage of combining cognitive neuromodulation interventions with neuroimaging during the early stages of clinical translation. The advantage of this multi-modal approach is that it offers a better understanding of the intervention mechanism, leading to a more precise characterization of inter-individual variation in intervention response. The results provide insights into the role of phase-amplitude coupling between lPFC and SMC in emotion control over social approach-avoidance behavior and contribute to developing targeted clinical interventions for anxiety.

Materials and Methods

Participants

Fifty-two highly socially anxious students (39 females) from Radboud University, Nijmegen, were recruited to participate in this pre-registered experiment (https://osf.io/j9s2z/). The local ethics committee approved the experiment (METC Arnhem-Nijmegen: CMO2014/288). We had to exclude 3 participants due to technical issues. Participants were selected based on high self-reported social anxiety levels, as detailed below, and screened on eligibility criteria, including no history of mental illness except anxiety disorders or current use of psychoactive medication. Additionally, we confirmed that participants had normal or corrected-to-normal vision and underwent screening for contraindications to magnetic resonance imaging (MRI) and non-invasive transcranial electrical stimulation. The mean age of the participants was 24.0 years, with an SD of ±4.3, and a range of 19 to 40.

Pre-screening took place using the Liebowitz Social Anxiety Scale (LSAS). Participants scoring 30 or higher (fear/anxiety and avoidance sub-scales combined) were included as this criterion provides an optimal balance between sensitivity and specificity in identifying individuals who meet the criteria for social anxiety disorder (*27*). This selection criterion resulted in an approximately normal distribution of LSAS scores within our study sample, with a mean of 64.4, a standard deviation (SD) of ±19.0, and a range from 31 to 106 (**Fig. 1A**). The trait sub-scale of the State-Trait Anxiety Inventory (STAI Y-2) was included to assess trait anxiety as an inter-individual difference marker of tACS BOLD dose-response, as endogenous prefrontal activation to the emotional action control challenge varies as a function of trait anxiety (*24*).

The current study in highly socially anxious individuals was designed to replicate the main finding of our previous investigation in healthy male students (*9*) that showed tACS phase- and dose-specific effects on emotional action control (https://osf.io/j9s2z/). This required a sample size that allowed us to detect the previously observed significant three-way interaction between Congruency (congruent, incongruent) * Stimulation (in-phase, anti-phase) * tACS-dose (BOLD signal in lPFC during stimulation *vs*. sham): $\eta_p^2 = 0.19$ (*9*). The minimum sample size required for this study to detect an effect of comparable magnitude is 45 participants (*a priori* sensitivity power analysis of RM-ANCOVA: $\alpha = .05$, power = .80, $\eta_p^2 = 0.19$; G*Power v3.1; (*42*)). Given that the current sample might be more heterogeneous due to mixed-sex and anxiety-related differences, and the precision of effect size estimates show regression towards the mean (*9*), we decided to increase our planned sample size to 50 participants.

Procedure

The data collection procedure spanned three separate days. On the first day, participants completed the Liebowitz Social Anxiety Scale (LSAS) and State-Trait Anxiety Inventory-Trait (STAI-trait, Y-2) questionnaires. Following this, participants underwent various scanning procedures, including a structural T1-weighted scan, a diffusion-weighted imaging scan (DWI, as reported in (*24*)), and a magnetic spectroscopy scan (MRS, as reported in (*24*)).

During the second and third days, neuronavigation was used to position the electrodes over the sensorimotor cortex (SMC) and lateral prefrontal cortex (lPFC). For details regarding electrode placement, please refer to the subsequent section. Subsequently, during both stimulation sessions, participants were inside the MR scanner. They performed a 5-minute practice task before proceeding to complete the approach-avoidance task with concurrent dual-site tACS and task-based functional MRI for approximately 35 minutes.

Approach-avoidance task

Emotional action control was manipulated using a validated social approach-avoidance task in which cognitive control is associated with lPFC-SMC theta-gamma coupling (*15*), and is sensitive to the phase-dependent effects of dual-site theta-gamma phase-amplitude tACS when controlling for inter-individual variation in prefrontal BOLD response to tACS (*9*). During functional MR scanning, participants lay inside the MR scanner with a joystick in their right hand resting on their lower abdomen. Participants were instructed to approach or avoid by moving the joystick toward or away from themselves, respectively. During the task, participants received written instructions on the screen (> 10 s) at the start of each block of 12 trials (~60 s) that stated, “Pull the joystick toward yourself when you see a happy face and push away from yourself when you see an angry face” (congruent condition), “Push the joystick away from yourself when you see a happy face and pull toward yourself when you see an angry face” (incongruent condition). Congruent and incongruent conditions alternated between blocks in a pseudo-random fashion. Between blocks, there was an inter-block interval of > 20 s. Each trial started with a fixation cross (500 ms) followed by a face stimulus (100 ms) to which participants had to respond within 2 s. Joystick movements over 30% of the maximum movement range were considered valid responses. If a participant did

not respond, they would receive on-screen feedback stating, "You did not move the joystick far enough". Instructions and the inter-block interval lead to an ~30 s wash-out period between stimulation conditions. Each participant had 288 trials on each of the two testing days, yielding 576 observations (trials) in total, equally distributed over congruency (congruent, incongruent) and stimulation (in-phase, anti-phase, sham) condition combinations (96 trials per bin).

Dual-site tACS stimulation

Dual-site tACS was applied online during task performance inside the MRI scanner using two sets of concentric ring electrodes (inner disc: 25 mm ø; outer ring: 80 mm inner-ø, 100 mm outer-ø) (*43*). Current direction alternated (-1 mA to +1 mA) between each disc-ring electrode set to achieve a time-varying electrical field in theta-band (6 Hz) frequency over right-lPFC and gamma-band (75 Hz) tapered with a 6 Hz theta wave over left-SMC. The tACS-phase manipulation was achieved by phase-locking gamma-band power to peaks (in-phase) or troughs (anti-phase) of the theta-band signal. During sham blocks, there was an initial 10 s period of stimulation to match potential sensations related to the onset of stimulation, after which stimulation was terminated. Within a session, participants received all stimulation conditions (in-phase, anti-phase, sham) alternating in a pseudo-random fashion between stimulus blocks of 12 trials (~60 s), interleaved with periods of no stimulation (instructions between blocks; > 30 s), and never repeating the same stimulation condition for two consecutive blocks.

We used neuronavigation (Localite TMS Navigator; RRID: SCR_016126) for individualized targeting of left-SMC (MNI [-28, -32, 64]; (*9*, *15*)) and right-lPFC (MNI [26, 54, 0]; (*9*, *15*, *44*)) based on anatomical masks of regions of interest registered to individual T1-weighted scans acquired during the first session. After localization, electrodes were attached to the participant's scalp using Ten20 conductive paste (MedCaT). Inside the MR scanner, stimulation was delivered using two Neuroconn DC-Stimulator Plus stimulators (neuroConn; impedance < 10 kOhm; RRID: SCR_015520). Stimulators were placed inside a magnetically shielded box designed with electronics that filtered out RF pulses of the MR scanner and combined with a BrainAmp ExG MR amplifier (www.brainproducts.com) that allowed continuous monitoring of stimulation output during the session.

Modeling of stimulation currents

The electric field magnitude (mV/mm) at the cortical target sites was estimated using SimNIBS (version 4.0; (*45*)). The concentric ring electrode sets were modeled as the disc (25 mm ø) and outer ring electrode (80 mm inner-ø, 100 mm outer-ø) with the same center, using a 2-layer medium (2 mm silicone rubber on top of 2 mm saline gel). The electrode sets were positioned over lPFC ([38, 95, 60]) and SMC ([-36, -10, 90]) using the template head mesh of SimNIBS. For all media, we used standard conductivities provided by SimNIBS. Direct currents of 1 mA were modeled to flow between the center disc electrode and the outer ring. The model results of the electric field magnitude at the cortical surface for both target sites are shown in **Fig. 2A**.

MRI

All participants underwent magnetic resonance imaging using a 3T MAGNETROM

Prisma MR scanner (Siemens AG, Healthcare Sector, Erlangen, Germany), which has a 64-channel head coil with a top opening that allows the electrode wires to be routed out of the back of the scanner bore.

The scans obtained during the MR sessions were aligned with a standard brain atlas to guarantee a uniform field of view (FoV) throughout the days. Each scanning day involved taking around 1800 functional images using a multi-band 6 sequence, 2 mm isotropic voxel size, TR/TE = 1000 / 34 ms, flip angle = 60°, phase angle P >> A, including ten volumes with reversed phase encoding direction (A >> P) used to correct image distortions.

High-resolution structural images were acquired with a single-shot MPRAGE sequence using a GRAPPA acceleration factor of 2, TR/TE = 2400/2.13 ms, an effective voxel size of 1 mm isotropic, 176 sagittal slices, a distance factor of 50%, a flip angle of 8°, orientation A >> P, and a FoV of 256 mm.

Behavior analyses

To determine the phase-dependent effect of tACS on emotional action control, error rates were compared between congruent and incongruent trials while controlling for dose-dependent effects of tACS ('tACS-dose'). This three-way interaction (emotional action control * tACS-phase * tACS-dose) was assessed on congruency effects (congruent *vs.* incongruent) estimated from trial-by-trial responses through Bayesian mixed effects models using the *brms* package (*46*) implemented in the R (https://www.r-project.org/). Bayesian mixed effects models adhered to the maximum random effects structure by including random slopes, intercepts, and correlations that could vary across participants for all fixed effects (congruency- and stimulation conditions). Outputs of these models are log odds ('*b*'). The significance of effects is interpreted based on the 95% CI not including zero.

We hypothesized that the congruency effect in error rates would decrease for in-phase and increase for anti-phase stimulation and that the size of the effect per participant would depend on the BOLD effect of tACS *versus* sham, a measure of dose dependence that is orthogonal to the contrast of interest (in-phase *versus* anti-phase). These expectations were preregistered at the Open Science Framework: (https://osf.io/j9s2z/).

fMRI analyses – preprocessing

All processing of the images was performed using MELODIC 3.00 as implemented in FSL 6.0.0 (https://fsl.fmrib.ox.ac.uk; (*47*)). Images were motion-corrected using MCFLIRT (*48*), and distortions in the magnetic field were corrected using TOPUP (*49*). Functional images were rigid-body registered to the brain-extracted structural image using FLIRT (*48*). Registration to MNI 2 mm standard space was performed using the nonlinear registration tool FNIRT. Images were spatially smoothed using a Gaussian 5 mm kernel and high pass filtered with a cut-off that was automatically estimated based on the task structure. Independent component analysis was run with a pre-specified maximum of 100 components (*50*); these components were manually inspected to remove potential noise sources (*51*).

fMRI analyses – GLM

Emotional action control effects on whole-brain BOLD activation were estimated by contrasting incongruent trials (approach angry and avoid happy) with congruent trials (avoid angry and approach happy) across stimulation conditions (in-phase, anti-phase, sham). tACS effects on the whole-brain BOLD signal were estimated by comparing stimulation (in-phase and anti-phase) to sham across congruency conditions (congruent and incongruent). Individual estimates of prefrontal tACS-dose were extracted from the 98% peak activated voxel inside the Harvard-Oxford MNI-space dlPFC (middle frontal gyrus) mask registered to the individual T1-weighted image. We ran an exploratory analysis using whole-brain correlation between individual variation in STAI trait anxiety (Y-2) and tACS-dose contrast.

First- and second-level GLM analyses were performed in FSL 6.0.5 using FEAT (*52*). The first-level model included 12 task regressors: approach angry, approach happy, avoid angry, and avoid happy were modeled separately for each stimulation condition (in-phase, anti-phase, and sham). For each regressor, events covered the time interval from stimulus presentation until the corresponding onset of joystick movement. The following nuisance regressors were included in the GLM as nuisance covariates: estimated head translations and rotations (six regressors), temporal derivates of those translations and rotations (6 regressors), and global signal time series in white matter and cerebrospinal fluid (two regressors). We used fixed effects analyses implemented in FEAT to combine first-level models of the two separate stimulation sessions (*52*). Group-level effects were assessed using FLAME 1 with outlier de-weighting (*53*), making family-wise error-corrected cluster-level inferences using a cluster-forming threshold of $z > 2.3$. This threshold provides a false error rate of ~5 % when using FSL FLAME 1.

References

1. M. G. Craske, M. B. Stein, Anxiety. *The Lancet* **388**, 3048–3059 (2016).

2. A. Pittig, G. W. Alpers, A. N. Niles, M. G. Craske, Avoidant decision-making in social anxiety disorder: A laboratory task linked to in vivo anxiety and treatment outcome. *Behav. Res. Ther.* **73**, 96–103 (2015).

3. J. A. Rattel, S. F. Miedl, J. Blechert, F. H. Wilhelm, Higher threat avoidance costs reduce avoidance behaviour which in turn promotes fear extinction in humans. *Behav. Res. Ther.* **96**, 37–46 (2017).

4. P. F. Lovibond, C. J. Mitchell, E. Minard, A. Brady, R. G. Menzies, Safety behaviours preserve threat beliefs: Protection from extinction of human fear conditioning by an avoidance response. *Behav. Res. Ther.* **47**, 716–720 (2009).

5. S. Grover, W. Wen, V. Viswanathan, C. T. Gill, R. M. G. Reinhart, Long-lasting, dissociable improvements in working memory and long-term memory in older adults with repetitive neuromodulation. *Nat. Neurosci.* **25**, 1237–1246 (2022).

6. R. Polanía, M. A. Nitsche, C. Korman, G. Batsikadze, W. Paulus, The Importance of Timing in Segregated Theta Phase-Coupling for Cognitive Performance. *Curr. Biol.* **22**, 1314–1318 (2012).

7. B. C. Preisig, L. Riecke, M. J. Sjerps, A. Kösem, B. R. Kop, B. Bramson, P. Hagoort, A. Hervais-Adelman, Selective modulation of interhemispheric connectivity by transcranial alternating current stimulation influences binaural integration. *Proc. Natl. Acad. Sci.* **118**, e2015488118 (2021).

8. I. R. Violante, L. M. Li, D. W. Carmichael, R. Lorenz, R. Leech, A. Hampshire, J. C. Rothwell, D. J. Sharp, Externally induced frontoparietal synchronization modulates network dynamics and enhances working memory performance. *eLife* **6**, e22001 (2017).

9. B. Bramson, H. E. den Ouden, I. Toni, K. Roelofs, Improving emotional-action control by targeting long-range phase-amplitude neuronal coupling. *eLife* **9**, e59600 (2020).

10. K. Heuer, M. Rinck, E. S. Becker, Avoidance of emotional facial expressions in social anxiety: The Approach–Avoidance Task. *Behav. Res. Ther.* **45**, 2990–3001 (2007).

11. K. Roelofs, J. van Peer, E. Berretty, P. de Jong, P. Spinhoven, B. M. Elzinga, Hypothalamus–Pituitary–Adrenal Axis Hyperresponsiveness Is Associated with Increased Social Avoidance Behavior in Social Phobia. *Biol. Psychiatry* **65**, 336–343 (2009).

12. J. M. van Peer, P. Spinhoven, J. G. van Dijk, K. Roelofs, Cortisol-induced enhancement of emotional face processing in social phobia depends on symptom severity and motivational context. *Biol. Psychol.* **81**, 123–130 (2009).

13. B. Bramson, D. Folloni, L. Verhagen, B. Hartogsveld, R. B. Mars, I. Toni, K. Roelofs, Human Lateral Frontal Pole Contributes to Control over Emotional Approach–Avoidance Actions. *J. Neurosci.* **40**, 2925–2934 (2020).

14. S. B. J. Koch, R. B. Mars, I. Toni, K. Roelofs, Emotional control, reappraised. *Neurosci. Biobehav. Rev.* **95**, 528–534 (2018).

15. B. Bramson, O. Jensen, I. Toni, K. Roelofs, Cortical Oscillatory Mechanisms Supporting the Control of Human Social–Emotional Actions. *J. Neurosci.* **38**, 5739–5749 (2018).

16. B. Voytek, A. S. Kayser, D. Badre, D. Fegen, E. F. Chang, N. E. Crone, J. Parvizi, R. T. Knight, M. D'Esposito, Oscillatory dynamics coordinating human frontal networks in support of goal maintenance. *Nat. Neurosci.* **18**, 1318–1324 (2015).

17. J. Weber, A.-K. Solbakk, A. O. Blenkmann, A. Llorens, I. Funderud, S. Leske, P. G. Larsson, J. Ivanovic, R. T. Knight, T. Endestad, R. F. Helfrich, Ramping dynamics and theta oscillations reflect dissociable signatures during rule-guided human behavior. *Nat. Commun.* **15**, 637 (2024).

18. R. M. G. Reinhart, J. A. Nguyen, Working memory revived in older adults by synchronizing rhythmic brain circuits. *Nat. Neurosci.* **22**, 820–827 (2019).

19. I. Volman, K. Roelofs, S. Koch, L. Verhagen, I. Toni, Anterior Prefrontal Cortex Inhibition Impairs Control over Social Emotional Actions. *Curr. Biol.* **21**, 1766–1770 (2011).

20. K. Roelofs, A. Minelli, R. B. Mars, J. van Peer, I. Toni, On the neural control of social emotional behavior. *Soc. Cogn. Affect. Neurosci.* **4**, 50–58 (2009).

21. R. H. Phaf, S. E. Mohr, M. Rotteveel, J. M. Wicherts, Approach, avoidance, and affect: a meta-analysis of approach-avoidance tendencies in manual reaction time tasks. *Front. Psychol.* **5** (2014).

22. R. Kaldewaij, S. B. J. Koch, M. M. Hashemi, W. Zhang, F. Klumpers, K. Roelofs, Anterior prefrontal brain activity during emotion control predicts resilience to post-traumatic stress symptoms. *Nat. Hum. Behav.* **5**, 1055–1064 (2021).

23. R. C. Lapate, I. C. Ballard, M. K. Heckner, M. D'Esposito, Emotional Context Sculpts Action Goal Representations in the Lateral Frontal Pole. *J. Neurosci.* **42**, 1529–1541 (2022).

24. B. Bramson, S. Meijer, A. van Nuland, I. Toni, K. Roelofs, Anxious individuals shift emotion control from lateral frontal pole to dorsolateral prefrontal cortex. *Nat. Commun.* **14**, 4880 (2023).

25. M. Feurra, P. Pasqualetti, G. Bianco, E. Santarnecchi, A. Rossi, S. Rossi, State-Dependent Effects of Transcranial Oscillatory Currents on the Motor System: What You Think Matters. *J. Neurosci.* **33**, 17483–17489 (2013).

26. P. Ruhnau, T. Neuling, M. Fuscá, C. S. Herrmann, G. Demarchi, N. Weisz, Eyes wide shut: Transcranial alternating current stimulation drives alpha rhythm in a state dependent manner. *Sci. Rep.* **6**, 27138 (2016).

27. D. S. Mennin, D. M. Fresco, R. G. Heimberg, F. R. Schneier, S. O. Davies, M. R. Liebowitz, Screening for social anxiety disorder in the clinical setting: using the Liebowitz Social Anxiety Scale. *J. Anxiety Disord.* **16**, 661–673 (2002).

28. D. Folloni, J. Sallet, A. A. Khrapitchev, N. Sibson, L. Verhagen, R. B. Mars, Dichotomous organization of amygdala/temporal-prefrontal bundles in both humans and monkeys. *eLife* **8**, e47175 (2019).

29. M. Petrides, D. N. Pandya, Dorsolateral prefrontal cortex: comparative cytoarchitectonic analysis in the human and the macaque brain and corticocortical connection patterns. *Eur. J. Neurosci.* **11**, 1011–1036 (1999).

30. M. K. P. Joyce, M. Á. García-Cabezas, Y. J. John, H. Barbas, Serial Prefrontal Pathways Are Positioned to Balance Cognition and Emotion in Primates. *J. Neurosci.* **40**, 8306–8328 (2020).

31. M. K. P. Joyce, J. Wang, H. Barbas, Subgenual and Hippocampal Pathways in Amygdala Are Set to Balance Affect and Context Processing. *J. Neurosci.* **43**, 3061–3080 (2023).

32. S. Berboth, C. Morawetz, Amygdala-prefrontal connectivity during emotion regulation: A meta-analysis of psychophysiological interactions. *Neuropsychologia* **153**, 107767 (2021).

33. M. W. Eysenck, J. S. Moser, N. Derakshan, P. Hepsomali, P. Allen, A neurocognitive account of attentional control theory: how does trait anxiety affect the brain's attentional networks? *Cogn. Emot.* **0**, 1–18 (2022).

34. M. R. Krause, P. G. Vieira, J.-P. Thivierge, C. C. Pack, Brain stimulation competes with ongoing oscillations for control of spike timing in the primate brain. *PLOS Biol.* **20**, e3001650 (2022).

35. M. Wischnewski, I. Alekseichuk, A. Opitz, Neurocognitive, physiological, and biophysical effects of transcranial alternating current stimulation. *Trends Cogn. Sci.* **27**, 189–205 (2023).

36. D. J. L. G. Schutter, Cutaneous retinal activation and neural entrainment in transcranial alternating current stimulation: A systematic review. *NeuroImage* **140**, 83–88 (2016).

37. B. Asamoah, A. Khatoun, M. Mc Laughlin, tACS motor system effects can be caused by transcutaneous stimulation of peripheral nerves. *Nat. Commun.* **10**, 266 (2019).

38. L. Johnson, I. Alekseichuk, J. Krieg, A. Doyle, Y. Yu, J. Vitek, M. Johnson, A. Opitz, Dose-dependent effects of transcranial alternating current stimulation on spike timing in awake nonhuman primates. *Sci. Adv.* **6**, eaaz2747 (2020).

39. M. R. Krause, P. G. Vieira, B. A. Csorba, P. K. Pilly, C. C. Pack, Transcranial alternating current stimulation entrains single-neuron activity in the primate brain. *Proc. Natl. Acad. Sci.* **116**, 5747–5755 (2019).

40. S. Grover, R. Fayzullina, B. M. Bullard, V. Levina, R. M. G. Reinhart, A meta-analysis suggests that tACS improves cognition in healthy, aging, and psychiatric populations. *Sci. Transl. Med.* **15**, eabo2044 (2023).

41. C. Bradley, A. S. Nydam, P. E. Dux, J. B. Mattingley, State-dependent effects of neural stimulation on brain function and cognition. *Nat. Rev. Neurosci.* **23**, 459–475 (2022).

42. F. Faul, E. Erdfelder, A.-G. Lang, A. Buchner, G*Power 3: A flexible statistical power analysis program for the social, behavioral, and biomedical sciences. *Behav. Res. Methods* **39**, 175–191 (2007).

43. G. B. Saturnino, K. H. Madsen, H. R. Siebner, A. Thielscher, How to target inter-regional phase synchronization with dual-site Transcranial Alternating Current Stimulation. *NeuroImage* **163**, 68–80 (2017).

44. F.-X. Neubert, R. B. Mars, A. G. Thomas, J. Sallet, M. F. S. Rushworth, Comparison of Human Ventral Frontal Cortex Areas for Cognitive Control and Language with Areas in Monkey Frontal Cortex. *Neuron* **81**, 700–713 (2014).

45. O. Puonti, K. Van Leemput, G. B. Saturnino, H. R. Siebner, K. H. Madsen, A. Thielscher, Accurate and robust whole-head segmentation from magnetic resonance images for individualized head modeling. *NeuroImage* **219**, 117044 (2020).

46. P.-C. Bürkner, brms: An R Package for Bayesian Multilevel Models Using Stan. *J. Stat. Softw.* **80**, 1–28 (2017).

47. M. Jenkinson, C. F. Beckmann, T. E. J. Behrens, M. W. Woolrich, S. M. Smith, FSL. *NeuroImage* **62**, 782–790 (2012).

48. M. Jenkinson, P. Bannister, M. Brady, S. Smith, Improved Optimization for the Robust and Accurate Linear Registration and Motion Correction of Brain Images. *NeuroImage* **17**, 825–841 (2002).

49. J. L. R. Andersson, S. Skare, J. Ashburner, How to correct susceptibility distortions in spin-echo echo-planar images: application to diffusion tensor imaging. *NeuroImage* **20**, 870–888 (2003).

50. C. F. Beckmann, S. M. Smith, Probabilistic independent component analysis for functional magnetic resonance imaging. *IEEE Trans. Med. Imaging* **23**, 137–152 (2004).

51. L. Griffanti, G. Douaud, J. Bijsterbosch, S. Evangelisti, F. Alfaro-Almagro, M. F. Glasser, E. P. Duff, S. Fitzgibbon, R. Westphal, D. Carone, C. F. Beckmann, S. M. Smith, Hand classification of fMRI ICA noise components. *NeuroImage* **154**, 188–205 (2017).

52. M. W. Woolrich, B. D. Ripley, M. Brady, S. M. Smith, Temporal Autocorrelation in Univariate Linear Modeling of FMRI Data. *NeuroImage* **14**, 1370–1386 (2001).

53. A. Eklund, T. E. Nichols, H. Knutsson, Cluster failure: Why fMRI inferences for spatial extent have inflated false-positive rates. *Proc. Natl. Acad. Sci.* **113**, 7900–7905 (2016).

54. R. Scheeringa, P. Fries, K.-M. Petersson, R. Oostenveld, I. Grothe, D. G. Norris, P. Hagoort, M. C. M. Bastiaansen, Neuronal Dynamics Underlying High- and Low-Frequency EEG Oscillations Contribute Independently to the Human BOLD Signal. *Neuron* **69**, 572–583 (2011).

Acknowledgments

We thank Jesse Lam for his support with data collection.

Funding: This work was funded by a consolidator grant DARE2APPROACH, from the European Research Council (ERC_CoG_772337) awarded to KR and also supporting SM and BB; by a consortium grant from the Dutch Research Council INTENSE (NWO_Crossover_17619) and by (NWO_SSH_406.20.GO.020) awarded to IT and KR.

Author contributions:
Conceptualization: SM, BB, IT & KR
Methodology: SM, BB, IT & KR
Investigation: SM, BB
Visualization: SM, BB, IT & KR
Supervision: BB, IT & KR
Writing—original draft: SM, BB, IT & KR
Writing—review & editing: SM, BB, IT & KR

Competing interests: The authors declare that they have no competing interests.

Data and materials availability: All data needed to evaluate the conclusions in the paper are present in the paper. The data and analysis code for this study will be deposited in the Radboud Data Repository (https://data.ru.nl/).

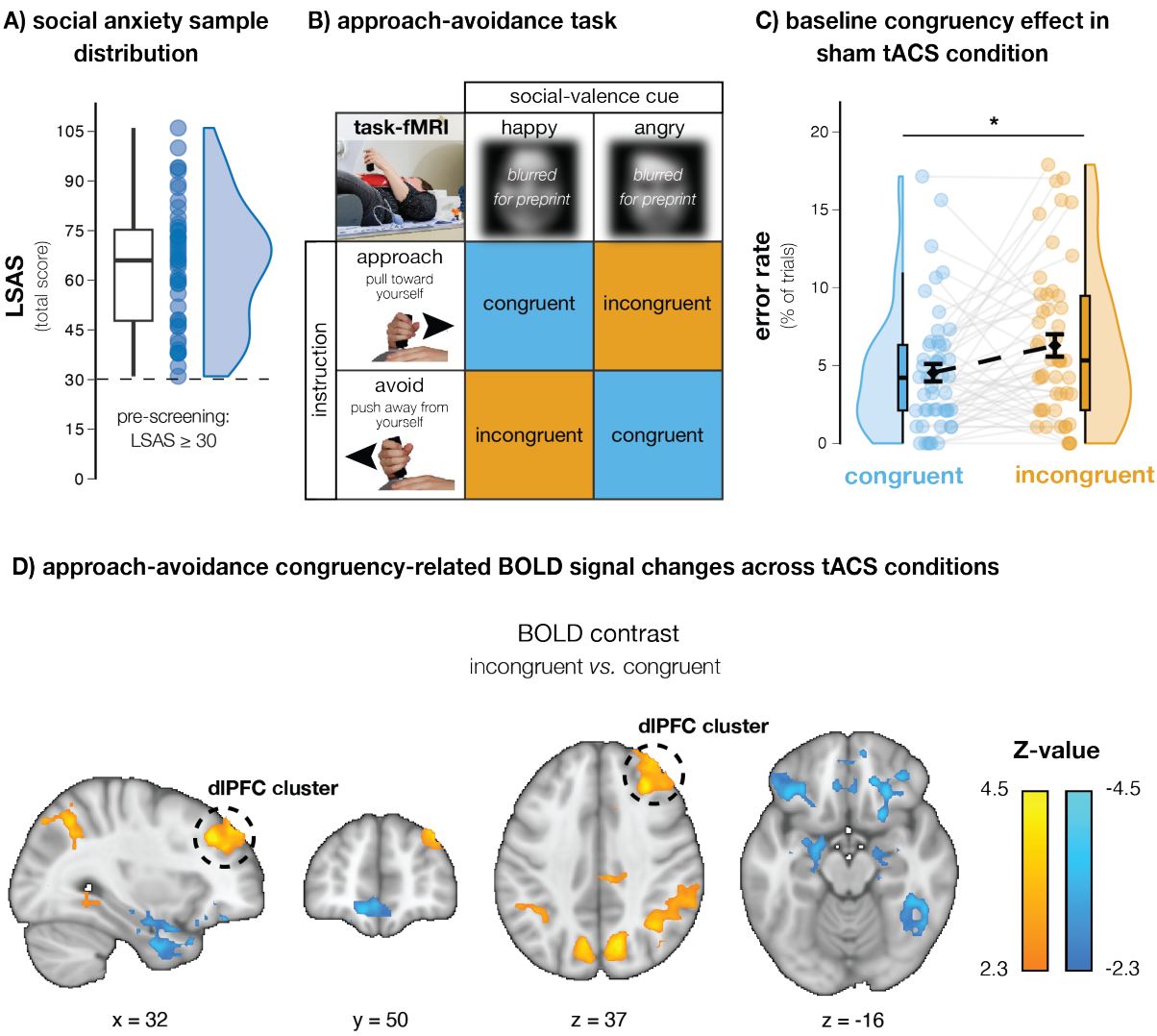

Fig. 1. Behavioral and BOLD fMRI effects related to control over emotional action tendencies. (A) *Sample distribution of self-reported Liebowitz Social Anxiety Scale (LSAS) scores. The black dashed line marks an LSAS score of 30, used to select socially anxious participants. This cut-off balances specificity and sensitivity in detecting social anxiety (27).* ***(B)*** *Conceptual visualization of the approach-avoidance task performed during concurrent dual-site tACS fMRI. In affect-congruent conditions, participants were instructed to pull the joystick towards them in response to a happy face and push it away from them in response to an angry face. In contrast, the affect-incongruent condition requires participants to override automatic emotional action tendencies to avoid angry and approach happy faces. Therefore, in this condition, participants were instructed to pull the joystick towards them in response to an angry face and push it away in response to a happy face.* ***(C)*** *Behavioral congruency-effects in the baseline sham stimulation condition of the task. Participants made more errors when overriding their automatic emotional action tendencies in the affect-incongruent condition (orange circles) as compared to making affect-congruent responses (blue circles), b = .41; 95% CI [.22 .61]. Black-filled diamonds represent mean values, and standard errors of the mean are shown with black lines.* ***(D)*** *Task-fMRI congruency-related effects across tACS stimulation conditions (incongruent > congruent; cluster-level inferences corrected for multiple comparisons). Stronger BOLD signals were observed in prefrontal- and parietal areas when automatic emotional action tendencies needed to be overridden, while amygdala-hippocampal and medial-orbitofrontal areas showed weaker BOLD signals.*

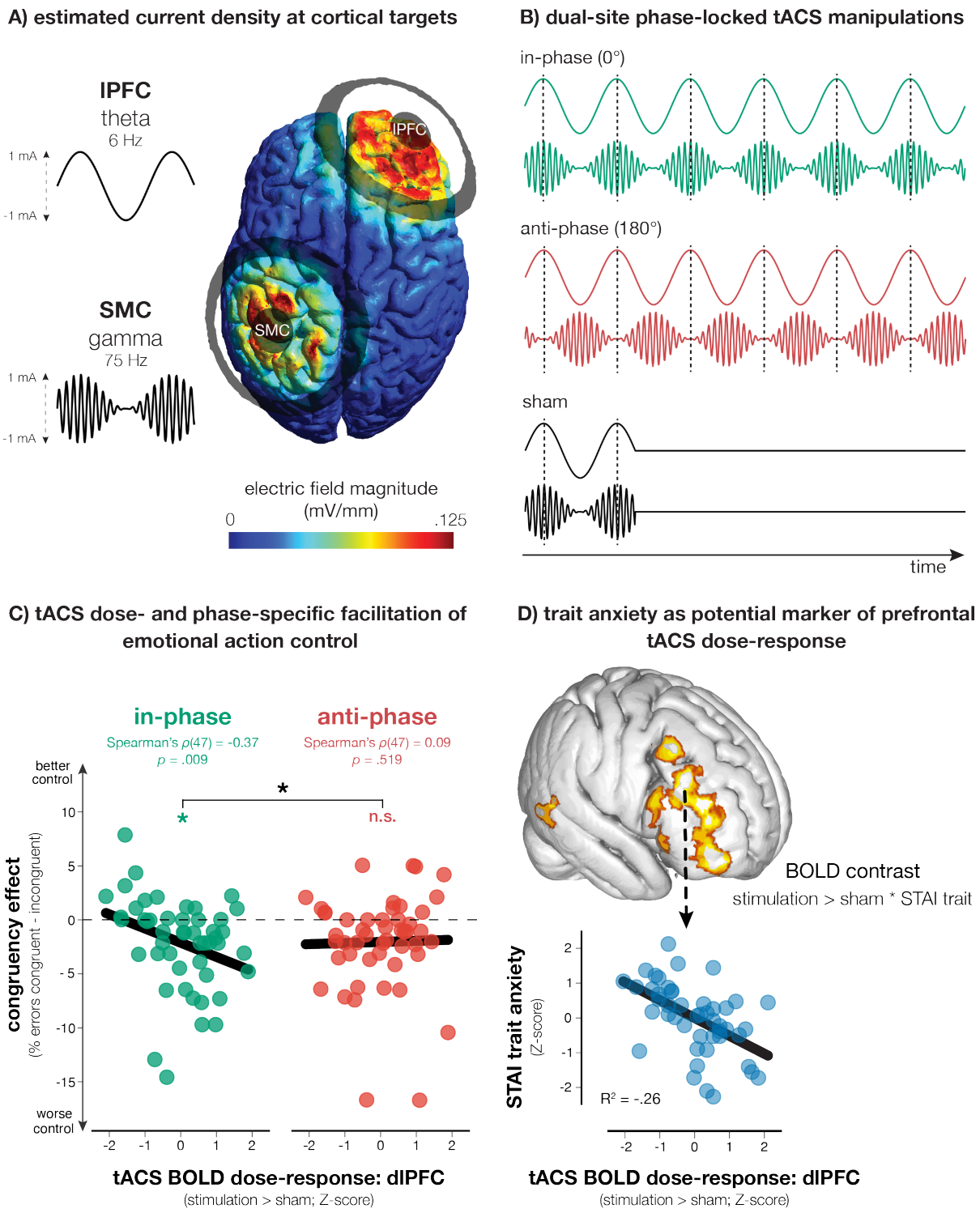

Fig. 2. Dose- and phase-specific effects of dual-site lPFC-SMC theta-gamma phase-amplitude coupled tACS on emotional action control in social anxiety. (A) *Two sets of concentric ring electrodes were placed over the right lPFC and left SMC. The current density model shows the spatial distribution of the electric field magnitude (mV/mm) evoked by the high-definition montage at both cortical targets, with intensities that can influence endogenous task-evoked oscillatory activity.* ***(B)*** *The stimulation conditions underwent a pseudo-random alternation throughout the experiment between in-phase, anti-phase, and sham conditions. Specifically, 75 Hz stimulation was administered over the SMC and its amplitude modulated by 6 Hz stimulation over the lPFC. Modulation was either in-phase or anti-phase with the*

peaks of the 6 Hz lPFC stimulation. The sham condition involved a brief 10-second initial stimulation that was discontinued before the start of the first trial. ***(C)*** *Participants showing more robust inhibitory responses to theta-band stimulation over dlPFC, evidenced by a decrease in blood-oxygen-level-dependent (BOLD) signal* (*9*, *54*)*, exhibited improved control over emotional actions (i.e., decreased congruency effect) during in-phase dual-site tACS (in green) compared to anti-phase dual-site tACS (in red), b = -.35; 95% CI [-.67 -.03] ([emotional action control (congruent, incongruent) * tACS-phase (in-phase, anti-phase) * tACS-dose dlPFC])*. ***(D)*** *Concurrent tACS-fMRI BOLD signal changes across in-phase and anti-phase tACS stimulation conditions correlated with trait anxiety, showing stronger dlPFC dose-response for individuals with higher trait anxiety levels.*